



HAL
open science

An 8 channel parallel transmit system with current sensor feedback for MRI-guided interventional applications

Felipe Godinez, Raphael Tomi-Tricot, Bruno Quesson, Matthias Barthel, Gunthard Lykowsky, Greig Scott, Reza Razavi, Joseph Hajnal, Shaihan Malik

► **To cite this version:**

Felipe Godinez, Raphael Tomi-Tricot, Bruno Quesson, Matthias Barthel, Gunthard Lykowsky, et al.. An 8 channel parallel transmit system with current sensor feedback for MRI-guided interventional applications. *Physics in Medicine and Biology*, 2021, 66, 10.1088/1361-6560/ac2fbc . hal-03869211

HAL Id: hal-03869211

<https://hal.science/hal-03869211>

Submitted on 24 Nov 2022

HAL is a multi-disciplinary open access archive for the deposit and dissemination of scientific research documents, whether they are published or not. The documents may come from teaching and research institutions in France or abroad, or from public or private research centers.

L'archive ouverte pluridisciplinaire **HAL**, est destinée au dépôt et à la diffusion de documents scientifiques de niveau recherche, publiés ou non, émanant des établissements d'enseignement et de recherche français ou étrangers, des laboratoires publics ou privés.

NOTE • OPEN ACCESS

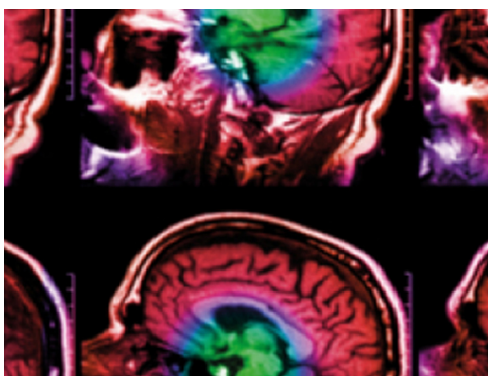
An 8 channel parallel transmit system with current sensor feedback for MRI-guided interventional applications

To cite this article: Felipe Godinez *et al* 2021 *Phys. Med. Biol.* **66** 21NT05

View the [article online](#) for updates and enhancements.

You may also like

- [Buckling prevention strategies in nature as inspiration for improving percutaneous instruments: a review](#)
Aimée Sakes, Dimitra Dodou and Paul Breedveld
- [Review—Voltammetric Sensors with Laterally Placed Working Electrodes: A Review](#)
Radosaw Porada, Katarzyna Jedlińska, Justyna Lipiska *et al.*
- [Silver nanoparticles functionalized Paclitaxel nanocrystals enhance overall anti-cancer effect on human cancer cells](#)
Nazim Muhammad, He Zhao, Wenjing Song *et al.*



IPEM | IOP

Series in Physics and Engineering in Medicine and Biology

Your publishing choice in medical physics,
biomedical engineering and related subjects.

Start exploring the collection—download the
first chapter of every title for free.



NOTE

An 8 channel parallel transmit system with current sensor feedback for MRI-guided interventional applications

OPEN ACCESS

RECEIVED
6 March 2021REVISED
29 September 2021ACCEPTED FOR PUBLICATION
14 October 2021PUBLISHED
1 November 2021

Original content from this work may be used under the terms of the [Creative Commons Attribution 4.0 licence](#).

Any further distribution of this work must maintain attribution to the author(s) and the title of the work, journal citation and DOI.



Felipe Godinez^{1,2,3,*}, Raphael Tomi-Tricot⁴, Bruno Quesson⁵, Matthias Barthel⁹, Gunthard Lykowsky⁷, Greig Scott⁸, Reza Razavi^{1,6}, Joseph Hajnal^{1,2} and Shaihan Malik^{1,2}

¹ School of Biomedical Engineering and Imaging Sciences, King's College London, London, United Kingdom

² Centre for the Developing Brain, King's College London, London, United Kingdom

³ Department of Radiology, University of California Davis, Sacramento, California, United States of America

⁴ MR Research Collaborations, Siemens Healthcare Limited, Frimley, United Kingdom

⁵ Centre de recherche Cardio-Thoracique de Bordeaux/IHU Liryc, INSERM U1045-University of Bordeaux, Pessac, France

⁶ Department of Congenital Cardiology, Evelina London Children's Healthcare, Guys and St Thomas' NHS Foundation Trust, London, United Kingdom

⁷ RAPID Biomedical GmbH, Rimpar, Germany

⁸ Magnetic Resonance Systems Research Laboratory, Department of Electrical Engineering, Stanford University, Stanford, California, United States of America

⁹ Barthel HF-Technik GmbH, Aachen, Germany

* Author to whom any correspondence should be addressed.

E-mail: fgodinez@ucdavis.edu

Keywords: parallel transmit MRI, vector modulation, add-on PTx system, MRI guided interventions, guidewire, Hilbert transform, MR safety

Supplementary material for this article is available [online](#)

Abstract

Background. Parallel transmit (pTx) has introduced many benefits to magnetic resonance imaging (MRI) with regard to decreased specific absorption rates and improved transmit field homogeneity, of particular importance in applications at higher magnetic field strengths. PTx has also been proposed as a solution to mitigating dangerous RF induced heating of elongated conductive devices such as those used in cardiac interventions. In this work we present a system that can augment a conventional scanner with pTx, in particular for use in interventional MRI for guidewire safety, by adjusting the amplitude and phase of each channel right before the start of the imaging pulses. **Methods.** The pTx system was designed to work in-line with a 1.5 T MRI while the RF synthesis and imaging control was maintained on the host MR scanner. The add-on pTx system relies on the RF transmit signal, unblanking pulse, and a protocol driven trigger from the scanner. The RF transmit was split into multiple fully modulated transmit signals to drive an array of custom transceiver coils. The performance of the 8-channel implementation was tested with regards to active and real-time control of RF induced currents on a standard guidewire, heating mitigation tests, and anatomical imaging in sheep. **Results.** The pTx system was intended to update RF shims in real-time and it was demonstrated that the safe RF shim could be determined while the guidewire is moved. The anatomical imaging demonstrated that cardiac anatomy and neighbouring superficial structures could be fully characterized with the pTx system inline. **Conclusion.** We have presented the design and performance of a real-time feedback control pTx system capable of adding such capabilities to a conventional MRI with the focus of guidewire imaging in cardiac interventional MRI applications.

1. Introduction

In cardiovascular interventions, magnetic resonance imaging (MRI) provides many benefits over standard x-ray fluoroscopy. However, not all interventional devices are MRI safe or can be visualized in MRI. Elongated conductive devices, such as guidewires, that are not ferromagnetic can still cause tissue burns at the proximal tip

driven by radiofrequency (RF) induced currents (Dempsey *et al* 2001, Buecker 2006), a phenomenon caused by the RF coupling between the transmit coil and the interventional device. A proposed solution is to manipulate the incident electric fields responsible for generating RF induced currents in implanted wires (McElcheran *et al* 2015, Eryaman *et al* 2019, Winter *et al* 2020), such that the net electric field tangential to the wire is forced to zero, consequently eliminating the potential for localized heating at the tip. This is possible using parallel transmit (pTx) MR systems which allow spatial manipulation of RF fields by altering the relative amplitude/phase of the individual transmitters. Using a two-channel birdcage coil (Eryaman *et al* 2011) demonstrated that a plane through a point on the implanted device with zero electric field could be achieved. Gudino *et al* (2015) demonstrated a similar approach on a guidewire using an eight channel pTx system. Both methods made use of a numerical model to determine the safe amplitude and phase weightings applied to each channel (RF shim). However, during interventions the RF coupling to the guidewire is constantly changing (Armenian *et al* 2004), which requires updating the safe RF shim in real-time to guarantee safety. A proposed solution is to predict the safe RF shim based on a quick measurement instead of a numerical prediction. Etezadi-Amoli *et al* (2015) proposed a fast method for computing intrinsically safe RF shims [coined the null modes (NM)] based on measurements made directly on the guidewire using a toroidal current sensor (Zanchi *et al* 2010). The same method also produces an unsafe RF shim, coined the coupling mode (CM) that if used carefully can be leveraged to visualize the guidewire (Godinez *et al* 2020). To achieve clinical translation this technique would require a pTx system with a real-time feedback control and be able to operate seamlessly with a conventional MRI scanner.

MRI scanners for investigational purposes, with pTx capability, have been built (Hebrank *et al* 2007, Vernickel *et al* 2007). The requirement for a bespoke engineered pTx enabled MRI system for investigation of interventional MRI is a barrier to advancement of this methodology. An approach is to design a system that can augment a conventional MRI scanner with pTx functionality for research purposes. One can augment the RF transmit subsystem only and rely on the host scanner to retain overall control of the imaging experiment. Examples of such ‘add-on’ pTx systems include a 32-channel system for a 7 T scanner (Orzada *et al* 2019) and a 64 channel system (Feng *et al* 2012).

This work presents the design and build of a similar ‘add-on’ pTx system designed for interventional MRI applications, implementing the techniques described in Etezadi-Amoli *et al* (2015), Godinez *et al* (2020). The key feature of this system is the ability to provide real-time RF current control by applying RF shims that can be updated during a continuing MR image acquisition. Firstly, the system design is presented in detail, followed by the calibrations used and pertinent methodology, and finally its performance is demonstrated in phantoms and an animal model in the context of interventional MR. The scope of this work is limited to the presentation of the pTx system as a useful device to investigate questions relevant to interventional MR and not to make a comparison with other systems or methods.

2. Methods

2.1. System overview

The proposed system is designed to connect transparently to a conventional MRI scanner with minimal required connections, so that the RF synthesis, sequence control, and data acquisition is kept by the host scanner. Meanwhile the pTx system controls the RF subsystem, by levelling and splitting the RF from the scanner across multiple transmit channels and then independently modulating the amplitude and phase of these (figure 1). Periodic measurements, once every imaging frame, from a current sensor are used to update the RF shim during a scan. The system is intended to perform RF shimming only; it can alter the amplitude/phase of each transmit channel for all RF pulses, but not change the ‘shape’ of the pulse waveforms, which are instead controlled by the scanner. The RF shim is fixed within a repetition time (TR) period.

To achieve these design goals, access to the scanner’s synthesized RF source, programmed pulse sequence trigger output, and the RF power amplifier (RFPA) unblank output are required. The pTx system replicates and modulates the RF signal from the scanner. The pulse sequence trigger initiates the current sensor measurements. The unblank signal is required to toggle the pTx system’s RF amplifiers on and off during transmit periods.

A further design requirement is that when ‘active’ the device should be ‘transparent’ to the scanner, so that automated power adjustments and pulse sequences from the scanner operate normally. This was accomplished by setting the overall gain of the pTx system to unity relative to the scanner. Unit gain was achieved by attenuating the RF signal before the 8 way split so that the RFPA output after the split can produce an excitation field level needed to carry out the automatic adjustments.

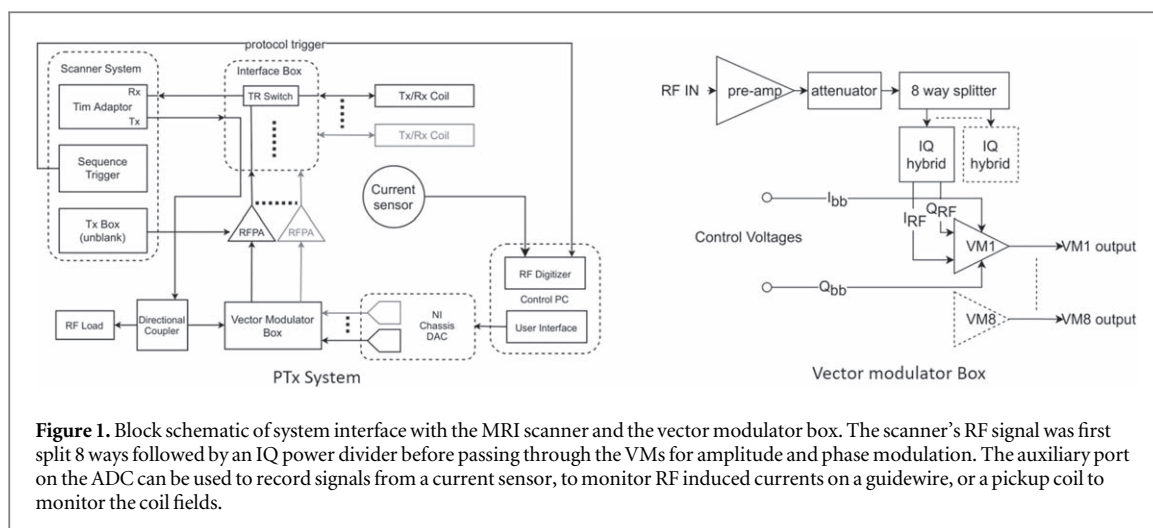


Figure 1. Block schematic of system interface with the MRI scanner and the vector modulator box. The scanner's RF signal was first split 8 ways followed by an IQ power divider before passing through the VMs for amplitude and phase modulation. The auxiliary port on the ADC can be used to record signals from a current sensor, to monitor RF induced currents on a guidewire, or a pickup coil to monitor the coil fields.

2.2. System implementation

The system as implemented has 8 transmit channels and was designed primarily to interface with a Siemens 1.5 T MRI system (MAGNETOM Aera, Siemens Healthcare, Erlangen, Germany) using standard connections, though it has also been connected to other scanners as detailed below.

2.2.1. RF coil interface and power amplification

The system connects to the scanner's local transmit coil socket, known as the total imaging matrix ('Tim') adaptor, located on the patient bed. The connection is made via an 'interface box' (figure 1) that connects to the transceiver coil. Use of the local transmit coil socket on the scanner causes the built-in body coil to be detuned and the (high power) RF signal to be routed to the Tim adaptor, and into the interface box. From here the high power signal is sent to a dummy RF load with 3 kW capacity, via a directional coupler (C9698-23, 3 kW, Werlatone Inc., NY, USA); the attenuated (-40 dB) 'forward power' port on this device is the input to our vector modulation stage, described in section 2.2.3.

After modulation the individual channel low-power RF signals are each amplified by an RFPA (Barthel HF-Technik GmbH, Aachen, Germany). The RFPAs each have a peak power limit of 1 kW and flexible 'energy control' capability allowing for 10% duty cycle at peak power, scaling linearly down to 100 W power output at continuous wave operation.

Finally, the amplified and modulated high power RF signals are sent back to the interface box where they are routed via transmit-receive switches to the RF coils. Since the RFPAs and the control computer are located in the control room, all connections are passed through the faraday cage filter panel. The RF load is located in the technical room.

2.2.2. Transceiver coil array

This work used a custom transceiver surface coil array designed and built by RAPID Biomedical (Rimpar, Germany) who also supplied the interface box (figure 2(a)). As well as handling the high-power RF as described above, this interface box routes the received signals via the scanner's standard receiver path. The transceiver has two surface coil arrays (anterior and posterior) each consisting of four $50\text{ mm} \times 200\text{ mm}$ rectangular loops with no overlap. Nearest and second-nearest-neighbor coil elements were capacitively decoupled.

2.2.3. Vector modulation

The attenuated RF signal coming from the scanner is levelled, using a pre-amp (25 dB) (ZHL-6A+, Mini-Circuits, Brooklyn NY, USA) and a variable attenuator (AC701, Pascall Electronics Limited, UK), before being split eight ways (ZCSC-8-1+, Mini-Circuits, Brooklyn NY, USA). Each of the eight signals are passed through a quad hybrid (PSCQ-2-180+, Mini-Circuits, Brooklyn NY, USA) to produce the in-phase (I) and quadrature (Q) signals needed for quadrature modulation using a vector modulator (VM; ADL5390, Analog Devices, Norwood, MA, USA)—evaluation boards were used. Figure 1 shows the block diagram for the network of VMs, which are housed in 3U 19" box, 'VM box' (figure 2(b)).

A total of 16 independent baseband control voltages $[I_{bb}, Q_{bb}]$ are required (two per channel) by the VMs, and these are supplied by an 8 bit digital-to-analog converter (DAC) card (PXI-6713, National Instruments, USA) mounted on a PXI chassis (PXI-1033, National Instruments, USA) connected to a PC (control PC)

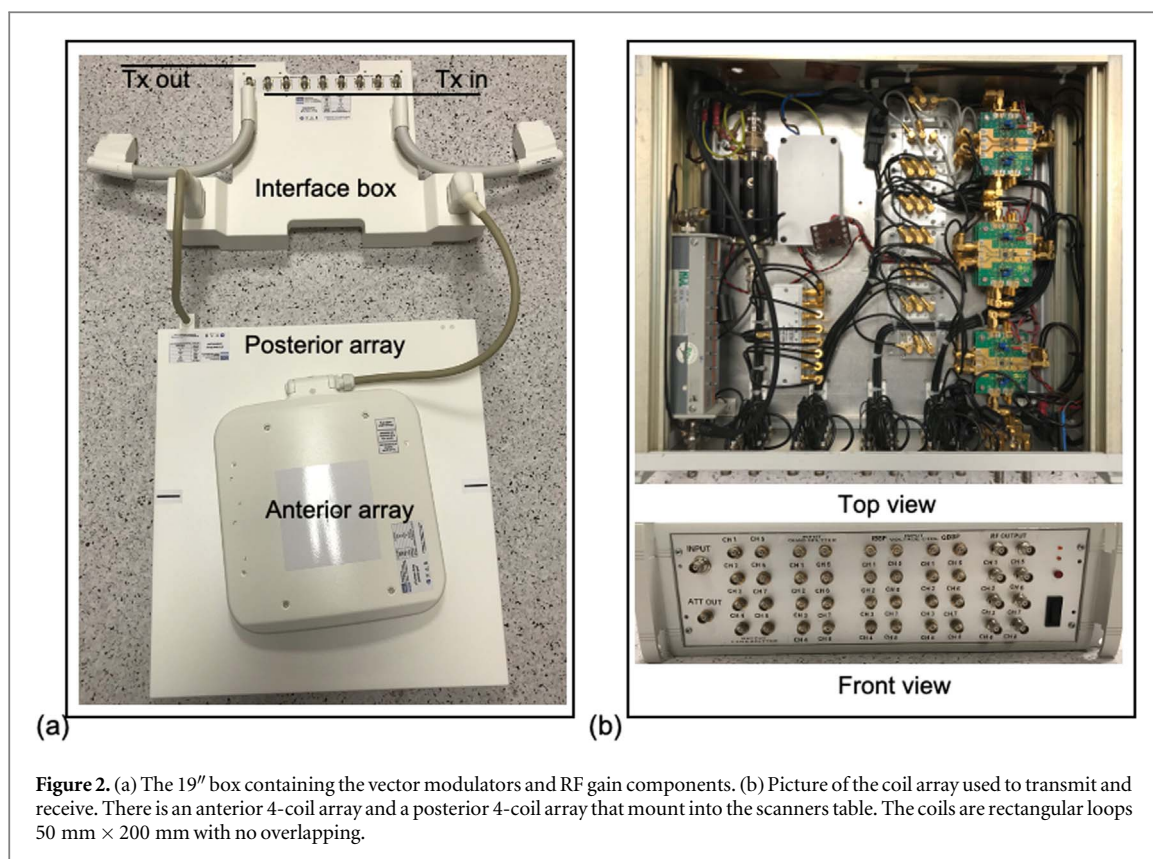


Figure 2. (a) The 19" box containing the vector modulators and RF gain components. (b) Picture of the coil array used to transmit and receive. There is an anterior 4-coil array and a posterior 4-coil array that mount into the scanners table. The coils are rectangular loops 50 mm \times 200 mm with no overlapping.

running Windows 7. The DAC produces a voltage range of ± 1.6 V; required $[I_{bb}, Q_{bb}]$ inputs are centered at 0.5 V (0–1 V range), such that a setting of [0.5, 0.5] produces zero at the VM output.

2.2.4. Current sensor

The feedback control loop is achieved by monitoring induced currents via a toroidal coil placed around the segment of the guidewire that is external to the patient's body, close to the entry point. This sensor was built from 1 mm diameter transformer wire coiled along the long-axis direction through a 5 mm diameter plastic tube, providing space for the guidewire to pass through. The sensor was wrapped with copper foil to block incident RF energy and a 10 m shielded balanced twin-pair line was attached to the coil and connected to a balun. The RF signal from the current sensor is digitized using a four-channel analog-to-digital converter (ADC) (PCI-Gage RMX-161-G40, Dynamic Signals LLC, USA) housed within the control PC. Direct and asynchronous signal demodulation based on the Hilbert transform was used, see section 2.3.1. The values recorded at the ADC are reported in volts as the current sensor calibration was omitted.

2.3. Control architecture

The pTx system performed a calibration, to form the coupling matrix C , at the beginning of the running imaging frame by measuring the RF coupling between the guidewire and the individual transmit coils with the current sensor. The calibration was initiated by the pulse sequence trigger followed by a 20 ms block RF pulse, during which the VM is used to cycle each channel on/off sequentially, while the current sensor output was recorded (figure 3). The complex current (amplitude and phase) measured in each cycle forms s_8 used to compute the coupling modes according to Etezadi-Amoli et al (2015). By applying the singular value decomposition to C the coupling modes were determined from the matrix of right-singular vectors V . Since this pTx system has 8 channels and 1 current sensor (up to 3 current sensors can be connected), 1 CM and 7 NM were computed, which was done within a 30 ms time window. If more sensors were used more than 1 CM mode might be found. The RF shim was set to either CM or NM by the user via the graphical user interface and was implemented in the next image frame. The user controls during acquisition are described in section 2.3.2.

2.3.1. Signal demodulation

Figure 3 summarizes the signal processing used to compute the coupling modes from the current sensor signal. A reference signal $R(t)$ from the transmit RF was digitized to perform asynchronous and direct demodulation of the current sensor signal $S(t)$ (Pérez et al 2001, Gareis et al 2006). The signal acquisition was under sampled at a

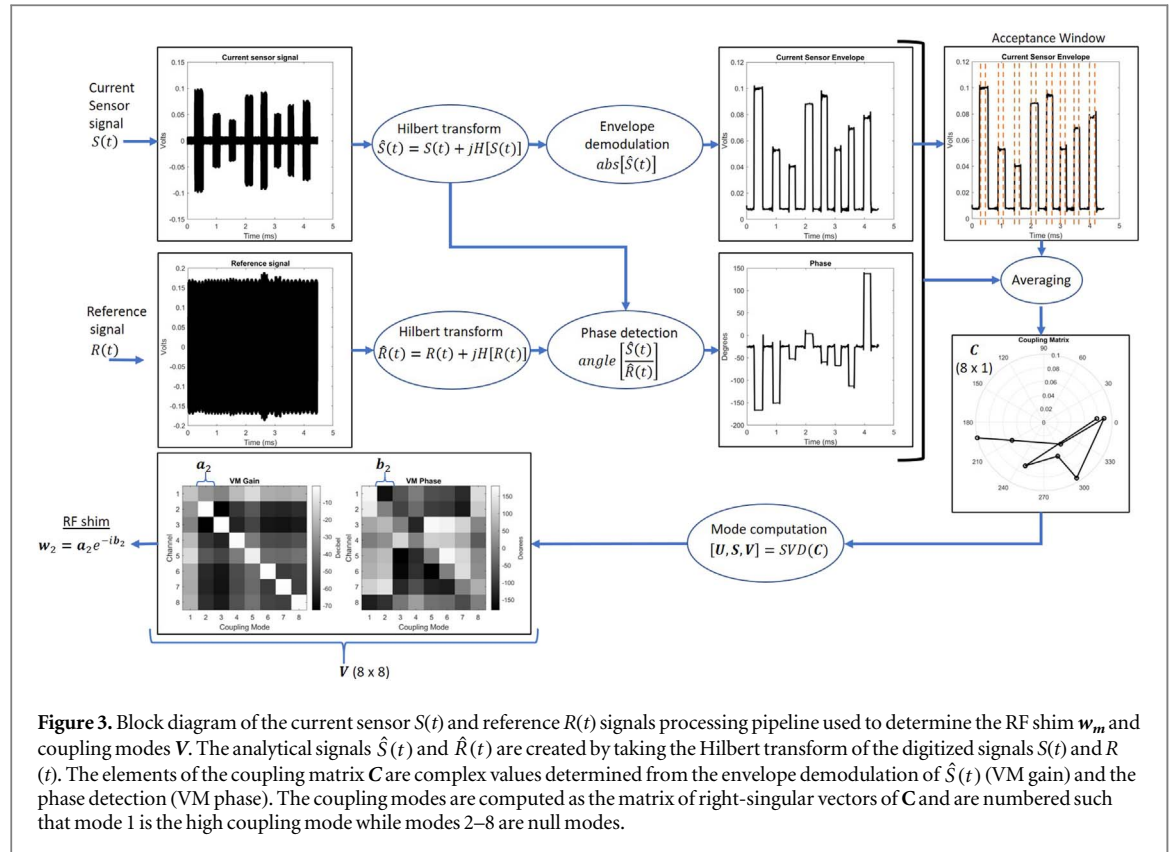


Figure 3. Block diagram of the current sensor $S(t)$ and reference $R(t)$ signals processing pipeline used to determine the RF shim w_m and coupling modes V . The analytical signals $\hat{S}(t)$ and $\hat{R}(t)$ are created by taking the Hilbert transform of the digitized signals $S(t)$ and $R(t)$. The elements of the coupling matrix C are complex values determined from the envelope demodulation of $\hat{S}(t)$ (VM gain) and the phase detection (VM phase). The coupling modes are computed as the matrix of right-singular vectors of C and are numbered such that mode 1 is the high coupling mode while modes 2–8 are null modes.

sample frequency of 500 kHz (RF frequency is 64 MHz). Envelope demodulation was performed by computing the magnitude of the analytical signal, $\hat{S}(t)$, created by the Hilbert transform (Xiaozhou *et al* 2019) of the digitized real valued signal, $S(t)$, as follows;

$$\hat{S}(t) = S(t) + jH[S(t)]$$

and

$$m(t) = abs[\hat{S}(t)],$$

where $m(t)$ is the envelope of $S(t)$. The phase $\phi(t)$ of $S(t)$ was obtained relative to the reference signal $R(t)$ by complex division, as

$$\phi(t) = \tan^{-1} \left[\frac{\hat{S}(t)}{\hat{R}(t)} \right].$$

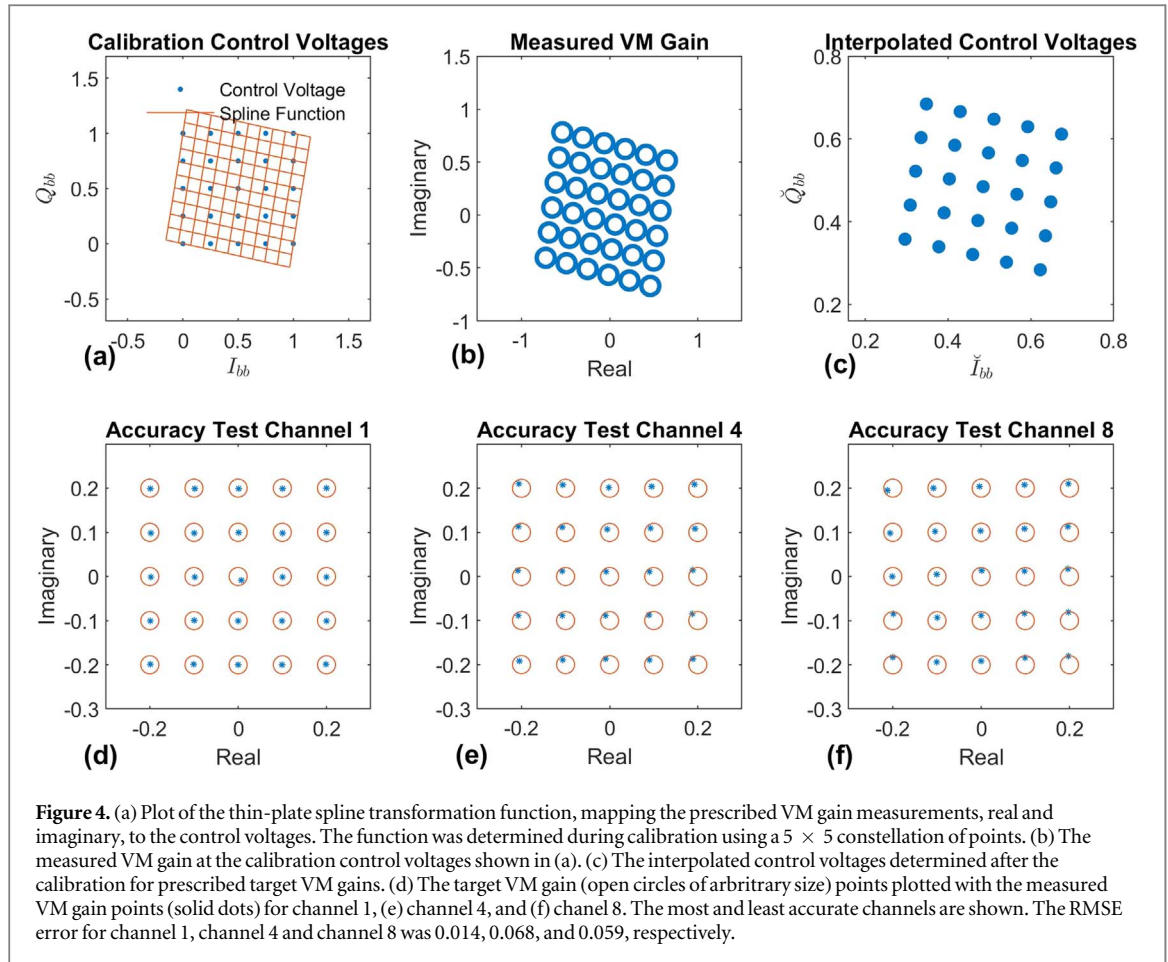
Since the system is controlled by a PC and not a real-time computer, the switching of the VMs occurs with variable timing. Hence, an edge detection algorithm was employed to set an acceptance window corresponding to each channel section. Once split, the signal was averaged to attain the final value of the amplitude and phase per channel, which make up the elements of the coupling matrix C .

2.3.2. Software

The stand-alone system is controlled by a PC running Windows 7. Software to control these devices was written in MatLab R2015b (MathWorks Inc., MA, USA), interfaced via a GUI. Its main functions are:

- (i) Pre-calibration to correct for nonlinear response of the VMs.
- (ii) Control of VM voltages to each channel for RF-shimming.
- (iii) Measurement of the current sensors, including demodulation.
- (iv) RF shims computation and mode selection by the user.
- (v) Monitoring and responding to the pulse sequence trigger.

Since the control software can set the amplitude and phase modulation applied to each channel, it can also control the overall RF power independently of the scanner's regulated transmit level.



2.4. Vector modulator calibration

VMs can produce a nonlinear response because of analog mixer imperfections and isolation errors in the splitting and combining networks at the inputs or outputs. Fortunately, this can be corrected via a feed-forward correction approach (Tošovský and Valúch 2010), which requires prior knowledge of the nonlinear distortions in the output gain and phase. Using this approach, the VMs were calibrated at the start of each session. The calibration consisted in determining a pre-distortion function; in this work a thin-plate spline function (Bookstein 1989, Padormo *et al* 2011) was used, which estimates the pre-distorted control voltages $[\check{I}_{bb}, \check{Q}_{bb}]$ that produce a desired VM output. The function for each VM was determined experimentally by measuring the VM gain and phase for an input 5×5 Cartesian grid of $[I_{bb}, Q_{bb}]$ values ranging from 0 to 1 V.

The fully automated calibration was done using a benchtop signal generator as a 64 MHz RF source and the ADC card to measure the amplitude/phase of the modulated signal. Subsequently, the thin-plate spline function was fit to the measured data. The thin-plate function used is,

$$f(\mathbf{x}) = \sum_{j=1}^{n-3} (|\mathbf{x} - \mathbf{c}_j|^2 \log |\mathbf{x} - \mathbf{c}_j|^2) a_j + x_1 a_{n-2} + x_2 a_{n-1} + a_n,$$

where $f(\mathbf{x})$ is a function that interpolates the control voltages $[\check{I}_{bb}, \check{Q}_{bb}]$ given the real and imaginary parts of the desired (the RF shim) VM gain and phase, handled as a complex point \mathbf{x} ($x_1 = \text{real}$, $x_2 = \text{imaginary}$). The variable n is the number of data points used during the calibration measurement, and \mathbf{c}_j is the complex Cartesian coordinate (real, imaginary) of the measured VM gain/phase. The polynomial coefficients $a_n, a_{n-1}, a_{n-2}, a_j$ are computed using the `tpaps(c,y)` function in MatLab which finds the minimizer f using the following cost function

$$E(f) = \sum_j |y(j) - f(\mathbf{c}(:,j))|^2,$$

where \mathbf{y} is a vector of test control voltages $[I_{bb}, Q_{bb}]$ chosen for the calibration to measure the VM gain, \mathbf{c} (figures 4(a), (b)). Using the function, f , the $[\check{I}_{bb}, \check{Q}_{bb}]$ needed for a prescribed RF shim can be determined by interpolating between the measured data points (figure 4(c)).

The accuracy of the calibration was tested by prescribing a set of RF shims and then measuring the resulting output for each channel (figures 4(d)–(f)). The average absolute RMS error between the prescribed RF shim and measured gain was computed for each channel using all the points in the Cartesian grid.

2.5. Real-time control

The system's ability to update the coupling modes in real-time was tested using a 3 T Achieva MRI scanner (Philips, The Netherlands) with a built-in 8-channel pTx transceiver array body coil (Vernickel *et al* 2007). This system was used for this test because the large built-in pTx body coil allowed a guidewire to be freely moved over a range of positions. In this experiment the add-on pTx system was connected in a similar manner as described above for a Siemens 1.5 T system, but directly to the pTx body coil present on the 3 T system, rather than the local array coil which was not used. The modulated transmit signals were amplified using the 3 T system's RFPAs. To operate at 3 T the hybrid splitters were swapped for counterparts at the desired frequency.

A straight guidewire (90 cm long nitinol guidewire, Terumo Corporation, Japan) was placed axially in the scanner's bore in air, instrumented with a toroidal current sensor. The test used a turbo spin echo sequence running at 100% reported specific absorption rate (SAR) with TR = 8 s, modified by adding the coupling matrix measurement block (30 ms) prior to each echo train. The software of the add-on pTx system could be set to either use this information to update the coupling mode calculation once per image (8 s) or ignore the new measurements and fix at a previous value.

A starting coupling matrix measurement was made with the guidewire placed at the left-hand edge of the scanner bed, position-A with the real-time control enabled. The guidewire was then moved to the right-hand bed edge, position-B, without updating the modes (i.e. real-time control disabled). After some acquisitions at position-B the real-time control was enabled to dynamically control the measured guidewire currents. The guidewire was then moved back to position-A from position-B while dynamically updating the coupling measurements. At each position and after each coupling measurement the NM and CM were applied in a random order. The temporal resolution of these measurements was determined by the TR period, 8 s in this case to allow the operator to move the guidewire between measurements. All measurements were run continuously and in the same experiment.

2.6. MR imaging

Imaging performance was evaluated on the Siemens 1.5 T MRI system mainly focused on torso imaging emulating interventional MR both in phantoms and *ex vivo*.

2.6.1. Heating tests

To demonstrate the efficacy of the pTx system to mitigate guidewire tip heating, a standard 0.89 mm diameter guidewire (RF + GA35153M, Terumo Corporation, Japan) cut to 140 cm length and stripped 3 mm at the tip, was equipped with a fiber-optic temperature probe (LumaSense Technologies, Inc. USA). The fiber-optic was tied directly onto the guidewire using suture string, making sure the guidewire was flush with the tip of the optical fiber. The guidewire was placed in a poly-acrylic acid gel phantom built according to (ASTM standard F 2182-2002a 2011) with the dimensions 45 cm × 36 cm × 9 cm. A high SAR balanced steady-state free precession (bSSFP) sequence was used to induce heating (Godinez *et al* 2020). The guidewire was located in the center of the phantom parallel to the static field and also centered with respect to the coil array.

2.6.2. Anatomical imaging

Anatomical images were obtained on a live sheep (44 kg) with a 164 cm long guidewire, to qualitatively evaluate system performance under realistic experimental conditions *in vivo*. The MR images were acquired with a bSSFP sequence with pixel size of 1.8 mm and TR/TE 2.70 ms/1.16 ms, using the NM RF shim or with the pTx system set with an RF shim of equal amplitude per channel and phased to achieve a nominal circular polarized mode (quad mode). All procedures involving animals were approved by the Animal Research Ethics Committee (CEEA 50—France) and performed in accordance with the European rules for animal experimentation.

3. Results

3.1. Vector modulator calibration

The observed distortion in the VM gain can be characterized as a rotation with a translation, see figure 4. After calibration the average RMSE across VM channels was 18% (min 6.8% and max 34.0%) of the dynamic range tested. The average absolute RMSE was 0.036 (min 0.014 and max 0.068). The greatest error was found in channels 4 and 8—in absolute values this was 0.068 and 0.059, compared to 0.014 for channel 1 (figures 4(e)–(f)). The RMSE error in channel 1 was 6.8%, calculated as a percent of the range.

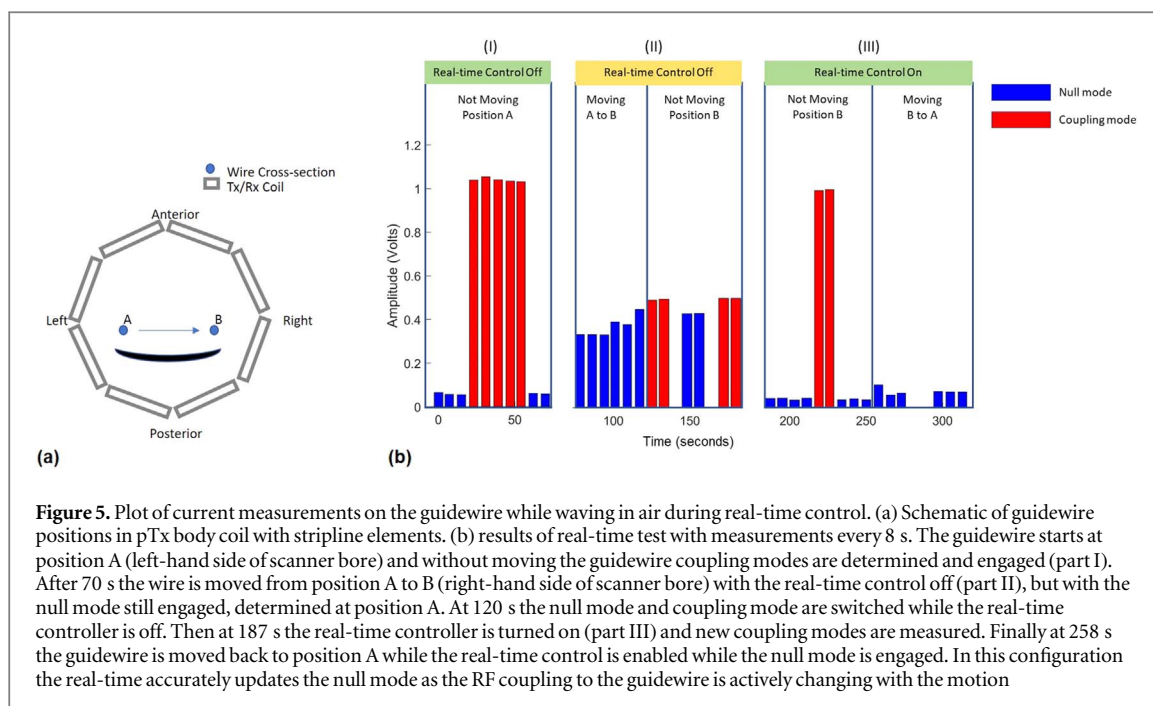


Figure 5. Plot of current measurements on the guidewire while waving in air during real-time control. (a) Schematic of guidewire positions in pTx body coil with stripline elements. (b) results of real-time test with measurements every 8 s. The guidewire starts at position A (left-hand side of scanner bore) and without moving the guidewire coupling modes are determined and engaged (part I). After 70 s the wire is moved from position A to B (right-hand side of scanner bore) with the real-time control off (part II), but with the null mode still engaged, determined at position A. At 120 s the null mode and coupling mode are switched while the real-time controller is off. Then at 187 s the real-time controller is turned on (part III) and new coupling modes are measured. Finally at 258 s the guidewire is moved back to position A while the real-time control is enabled while the null mode is engaged. In this configuration the real-time accurately updates the null mode as the RF coupling to the guidewire is actively changing with the motion

3.2. Real-time control

Figure 5 shows the real-time performance of the PTx system while moving a guidewire in air while switching between CM and NM, which should register high and low voltage measurements at the current sensor, respectively. The number of CM and NM acquisitions was done randomly, and in some cases the measurement failed because the control software was delayed, these measurements are shown as an empty time point. At the beginning of the experiment the real-time control is active and the wire is at position A (figure 5(b-I)); the CM shows current sensor values >1.0 V and the NM shows values <0.1 V, as expected. When the real-time control is disabled and the guidewire is moved from its original calibration position (figure 5(b-II)), the measured voltage is similar for both the CM (0.49 V) and NM (0.39 V). This means the RF coupling has changed and the induced current is uncontrolled. When it is enabled (figure 5(b-III)), the measurements follow the expected response from the CM (1.05 V) and NM (0.05 V), even when the guidewire is in motion. This test, using a wire in air, is not indicative of performance *in vivo*—the field changes experienced here are much more extreme—however it demonstrates that the feedback control mechanism is working as expected.

3.3. Heating test

Figure 6 shows the measured temperature at the guidewire tip in a phantom experiment while scanning with either the CM or NM at equivalent RF power. The measured temperature increase was reduced from 23.89 °C in CM to 1.65 °C in NM, demonstrating strong suppression of induced currents. During the NM the temperature did not fully return to baseline until the RF power was turned off. This may be a result of an imperfect calibration or inaccurate RF coupling estimation.

3.4. MR PTx imaging

The image shown in figure 7 demonstrates that standard anatomical imaging is possible while using the pTx system in quad mode and NM. During this scan the scanner completed its standard power scaling procedure and reported a reference voltage of 217 V (maximum allowed was 234 V). This demonstrates that when not actively controlled the system can operate under the full control of the host MR scanner.

4. Discussion

An auxiliary pTx system intended for interventional MRI, was assembled and proven to add parallel transmit capabilities to a non-pTx scanner. Its key function was to perform RF shimming, operating independently from the host scanner during imaging with real-time feedback control based on concurrent current measurements. The results indicate that when set to standard ‘quadrature’ mode the device can be used to produce images using standard protocols. Active control of induced currents on inserted guidewires was also demonstrated, with strong attenuation of temperature increases.

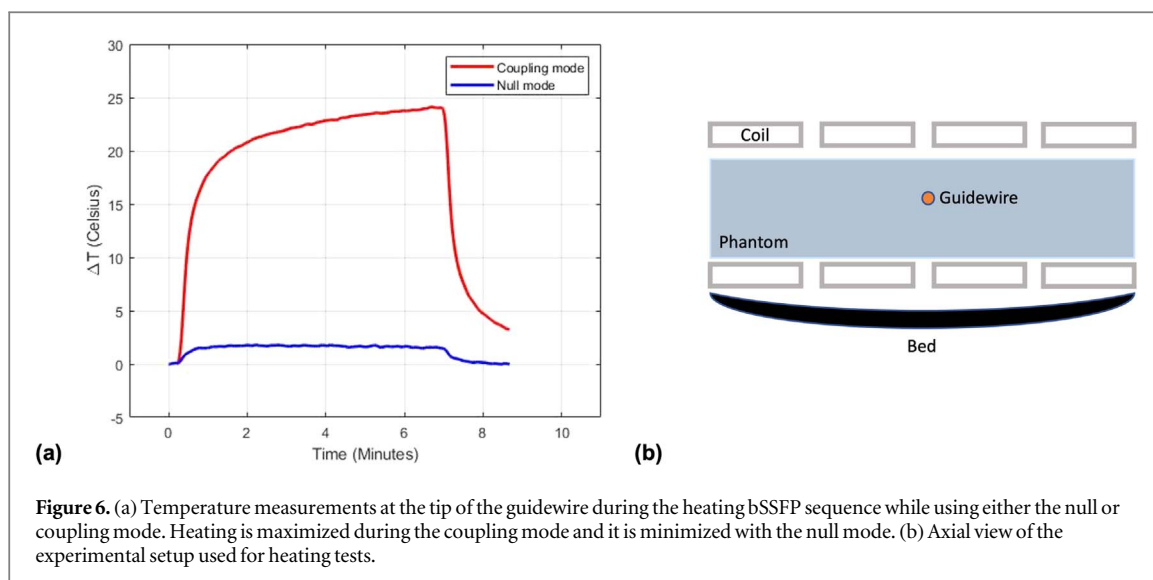


Figure 6. (a) Temperature measurements at the tip of the guidewire during the heating bSSFP sequence while using either the null or coupling mode. Heating is maximized during the coupling mode and it is minimized with the null mode. (b) Axial view of the experimental setup used for heating tests.

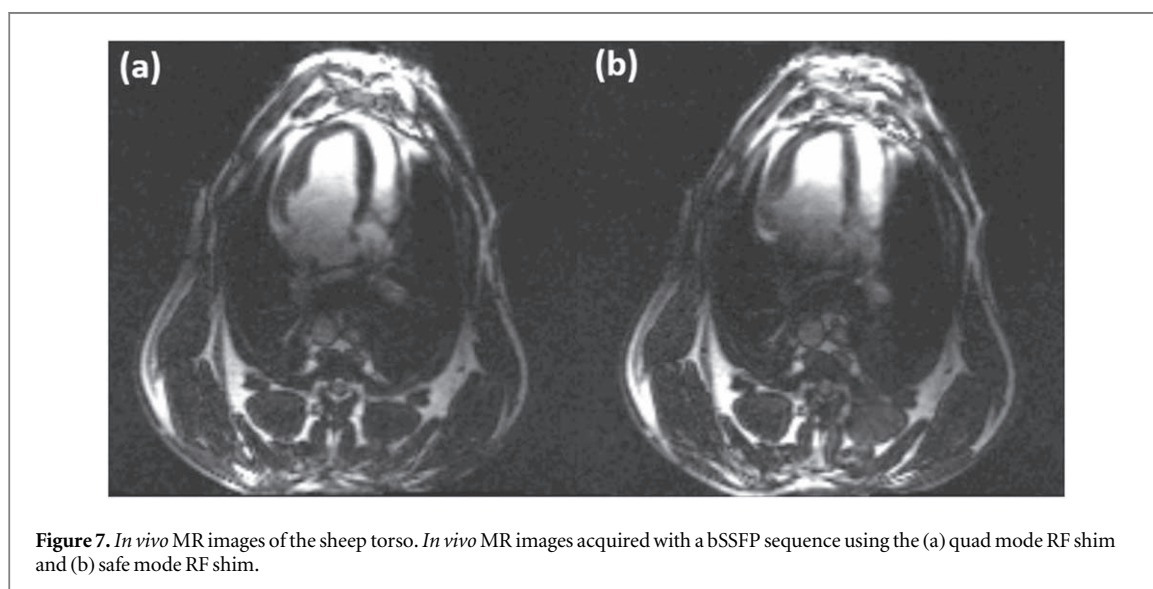


Figure 7. *In vivo* MR images of the sheep torso. *In vivo* MR images acquired with a bSSFP sequence using the (a) quad mode RF shim and (b) safe mode RF shim.

The maximum RMSE found in the VM calibration was 34%, which was mainly from channels 4 and 8. However, most of the channels performed better than this. The individual channel error might introduce inaccuracies to the overall RF shims, which may be observed as a non-zero induced current with the NM. Nonetheless, given the experimental results, the system can still perform well enough to reduce heating at the guidewire tip. The source of this error is not clear, but we speculate it comes from inter-channel coupling in the RF path.

This add-on pTx system was primarily designed for a 1.5 T application but was also connected to a 3 T scanner with non-standard body coil. Although the difference in field strength changes the resonant length of the guidewire, sufficient RF coupling to the 90 cm guidewire was found at 3 T to evaluate the pTx system's real time current control performance. In that case some narrow-band RF components (hybrid splitters and RFPAs) had to be swapped to the appropriate frequency. If such a system is required to work across frequencies, then broadband components could be selected where available—this was not a design requirement for the device as presented.

A limitation for this demonstration device is that SAR monitoring was not implemented, which would be a requirement for progression of this work to human imaging. The amplifiers used in this work did have integrated directional couplers and a digitization system that reported average forward and reflected power based on a short time window, and this could form the basis of a future SAR monitoring framework, as done by Orzada *et al* (2019).

In contrast to the system build by Feng *et al* (2012), our pTx system is relatively simple with fewer channels. Some applications may need more than eight channels for the system to be effective. Compared to the system

presented by Orzada *et al* (2019), our system is more portable but lacks the ability to do dynamic shimming, a feature that might increase its utility for more complex protocols and device safety methods. Although dynamic shimming is possible at base band signals with a bandwidth less than 1.85 kHz, it would not be sufficient to handle complete RF pulse envelope modulation (Orzada *et al* 2019), which could demand bandwidths of 100 kHz or more. Since the DAC card in this build has a sampling rate of up to 769 kS s^{-1} per channel, the bandwidth bottle neck is the operating system priority control. The average interval between VM control voltage updates was $274 \pm 50 \mu\text{s}$. The absence of a real-time operating system imposes a non-deterministic performance on the system, barring the direct shaping of RF pulses and causing coupling matrix measurements to fail, as seen in the dynamic test.

The presented pTx system is intended for further development of interventional MRI using endovascular guidewires. In this design a single toroidal current sensor was used to measure currents. In the future this could be expanded to multiple sensors or other sensors that provide relevant real-time information. These sensors should also be compact and sterilizable to be integrated in current clinical practice, to be placed over the external end of a guidewire.

The demonstrated anatomical imaging revealed lower signal at the centre of the field of view because of the use of surface coils that have strongly surface-weighted sensitivity. The loss of signal strength might also reduce the electric field, but not to the extent that RF coupling is insignificant (see supporting information figure 1 (available online at stacks.iop.org/PMB/66/21NT05/mmedia)). A method to improve image quality is to correct for receiver coil inhomogeneity (Murakami *et al* 1996), which was not done in this experiment but could be in future work. This issue might also be addressed by improved RF coil design; this is outside the scope of this work, which focused on the pTx control system development. It should also be noted that for interventional work the drop in standard imaging performance may still be acceptable should the system allow clinicians to perform hitherto unavailable procedures. In addition, it would be interesting to compare the local coil against a body coil to understand the impact on heating of the coil itself. This is the target of future work (Godinez *et al* 2021).

5. Conclusion

We have built an add-on pTx system that can be used to augment conventional MRI scanners to add pTx functionality for interventional MRI. The system is capable of RF shimming and functions transparently to the host MR system.

ORCID iDs

Felipe Godinez  <https://orcid.org/0000-0002-0951-8370>

References

- Armenean C, Perrin E, Armenean M, Beuf O, Pilleul F and Saint-Jalmes H 2004 RF-induced temperature elevation along metallic wires in clinical magnetic resonance imaging: influence of diameter and length *Magn. Reson. Med.* **52** 1200–6
- ASTM F2182-11a 2011 Standard test method for measurement of radio frequency induced heating near passive implants during magnetic resonance imaging *ASTM Int.* **1**–14
- Bookstein F L 1989 Principal warps: thin-plates splines and the decomposition of deformations *IEEE Trans. Pattern Anal. Mach. Intell.* **11** 567–85
- Buecker A 2006 Safety of MRI-guided vascular interventions *Minim. Invasive Ther. Allied Technol.* **15** 65–70
- Dempsey M F, Condon B and Hadley D M 2001 Investigation of the factors responsible for burns during MRI *J. Magn. Reson. Imaging* **13** 627–31
- Eryaman Y *et al* 2019 A simple geometric analysis method for measuring and mitigating RF induced currents on Deep Brain Stimulation leads by multichannel transmission/reception *Neuroimage* **184** 658–68
- Eryaman Y, Akin B and Atalar E 2011 Reduction of implant RF heating through modification of transmit coil electric field *Magnetic Resonance in Medicine* **1313** 1305–13
- Etezadi-Amoli M, Stang P, Kerr A, Pauly J and Scott G 2015 Controlling radiofrequency-induced currents in guidewires using parallel transmit *Magn. Reson. Med.* **74** 1790–802
- Feng K, Hollingsworth N A, McDougall M P and Wright S M 2012 A 64-channel transmitter for investigating parallel transmit MRI *IEEE Trans. Biomed. Eng.* **59** 2152–60
- Gareis D, Neuberger T, Behr V C, Jakob P M, Faber C and Griswold M A 2006 Application of undersampling technique for the design of an NMR signals digital receiver *Concepts Magn. Reson. B* **29B** 20–7
- Godinez F, Scott G, Hajnal J V and Malik S J 2021 Is a local Tx coil sufficient for guidewire safety in MRI? *Proc. Int. Soc. Mag. Reson. Med.* vol 29, p 2310
- Godinez F, Scott G, Padormo F, Hajnal J V and Malik S J 2020 Safe guidewire visualization using the modes of a PTx transmit array MR system *Magn. Reson. Med.* **83** 2343–55
- Gudino N *et al* 2015 Parallel transmit excitation at 1.5 T based on the minimization of a driving function for device heating *Med. Phys.* **42** 359–71

- Hebrank F X et al 2007 Parallel transmission (pTX) technology MR imaging with an 8-channel RF transmit array *Magnetom Flash* **1** 75–9
https://cdn0.scrvt.com/39b415fb07de4d9656c7b516d8e2d907/1800000000014352/e36c9da0902b/parallel_transmission_1800000000014352.pdf
- McElcheran C E, Yang B, Anderson K J T, Golestani-Rad L and Graham S J 2015 Investigation of parallel radiofrequency transmission for the reduction of heating in long conductive leads in 3 Tesla magnetic resonance imaging *PLoS One* **10** 1–21
- Murakami J W, Hayes C E and Weinberger E 1996 Intensity correction of phased-array surface coil images *Magn. Reson. Med.* **35** 585–90
- Orzada S et al 2019 A 32-channel parallel transmit system add-on for 7T MRI *PLoS ONE* **14** 1–20
- Padormo F, Malik S J, Mens G and Hajnal J V 2011 A method for calibrating multi-channel RF systems *Proc. Int. Soc. Mag. Reson. Med.* **19**, p 3858 <https://cds.ismrm.org/protected/11MProceedings/PDFfiles/3858.pdf>
- Pérez P, Santos A and Vaquero J J 2001 Potential use of the undersampling technique in the acquisition of nuclear magnetic resonance signals *Magn. Reson. Mater. Phys., Biol. Med.* **13** 109–17
- Tošovský P and Valúch D 2010 Improvement of RF vector modulator performance by feed-forward based calibration *Radioengineering* **19** 627–32
- Vernickel P et al 2007 Eight-channel transmit/receive body MRI coil at 3T *Magn. Reson. Med.* **58** 381–9
- Winter L et al 2020 Parallel transmission medical implant safety testbed: real-time mitigation of RF induced tip heating using time-domain E-field sensors *Magn. Reson. Med.* **84** 3468–84
- Xiaozhou L, Qianjuan W, Jingjing L and Haibin J 2019 Signal demodulation algorithm based on Hilbert transform and its application in aircraft power supply system characteristic parameters testing *2019 14th IEEE Int. Conf. Electron. Meas. Instruments, ICEMI 2019* pp 1549–54
- Zanchi M G, Venook R, Pauly J M, Scott G C and Member S 2010 An optically coupled system for quantitative monitoring of MRI-induced RF currents into long conductors *IEEE Trans. Med. Imaging* **29** 169–78